Carbohydrate Polymers 112 (2014) 677–685

Contents lists available at ScienceDirect

Carbohydrate Polymers

journal homepage: www.elsevier.com/locate/carbpol

Horse chestnut (*Aesculus hippocastanum* L.) starch: Basic physico-chemical characteristics and use as thermoplastic material

J. Castaño[a], S. Rodríguez-Llamazares[b,*], K. Contreras[b], C. Carrasco[c,**], C. Pozo[b], R. Bouza[d], C.M.L. Franco[e], D. Giraldo[f]

[a] Unidad de Desarrollo Tecnológico, Universidad de Concepción, Avda. Cordillera 2634, Coronel, Chile
[b] Centro de Investigación de Polímeros Avanzados (CIPA), Beltran Mathiew 224, Concepción, Chile
[c] Materials Engineering Department, Universidad de Concepción, Edmundo Larenas 270, Concepción, Chile
[d] Departamento de Física, E.U.P. Ferrol, Universidad de A Coruña, Avda. 19 de Febrero, s/n, 15405 Ferrol, Spain
[e] Departamento de Engenharia e Tecnologia de Alimentos, Universidade Estadual Paulista, R. Cristóvão Colombo, 2265 São José do Rio Preto, SP, Brazil
[f] Department of Metallurgical and Materials Engineering, Faculty of Engineering, University of Antioquia UdeA, Calle 70 No. 52-21, Medellín, Colombia

ARTICLE INFO

Article history:
Received 29 March 2014
Received in revised form 31 May 2014
Accepted 8 June 2014
Available online 28 June 2014

Keywords:
Aesculus hippocastanum L.
Amylopectin structure
Thermoplastic starch
Non-edible source

ABSTRACT

Starch isolated from non-edible *Aesculus hippocastanum* seeds *was* characterized and used for preparing starch-based materials. The apparent amylose content of the isolated starch was 33.1%. The size of starch granules ranged from 0.7 to 35 μm, and correlated with the shape of granules (spherical, oval and irregular). The chain length distribution profile of amylopectin showed two peaks, at polymerization degree (DP) of 12 and 41–43. Around 53% of branch unit chains had DP in the range of 11–20. *A. hippocastanum* starch displayed a typical C-type pattern and the maximum decomposition temperature was 317 °C.

Thermoplastic starch (TPS) prepared from *A. hippocastanum* with glycerol and processed by melt blending exhibited adequate mechanical and thermal properties. In contrast, plasticized TPS with glycerol:malic acid (1:1) showed lower thermal stability and a pasty and sticky behavior, indicating that malic acid accelerates degradation of starch during processing.

1. Introduction

The growing accumulation of plastic residues in landfills and oceans and the strong dependency of plastic production on fossil petroleum resources have stimulated research on bio-based plastic alternatives. Starch is a renewable and inherently biodegradable raw material of low-cost that can be transformed into bio-plastics with technologies currently used for manufacturing synthetic plastics. The worldwide production of starch-based plastics is estimated to exceed 150,000 tons/year (European Bioplastic, 2014).[1]

Thermoplastic starch (TPS) can be obtained by physical modification of starch, mixing starch with a plasticizer, with and without shear stress, at temperatures over 100 °C. Water, the main plasticizer of TPS, is used together with other plasticizers, such as polyols (sorbitol, xylitol, pentaerythritol and glycerol), sugar alcohols and non-ionic and anionic surfactants (Vieira, da Silva, dos Santos, & Beppu, 2011). There are many reports of starch coming from different botanical sources to prepare TPS. In most studies starch comes from edible fruits, vegetables, seeds and so on (van Soest, Benes, de Wit, & Vliegenthart, 1996; Zullo & Iannace, 2009). The use of edible sources for fabrication of plastics is controversial, especially in developing countries with a deficit of arable land and food. Therefore, non-edible starch has gained much attraction for use in starch-based materials (Bharadwaj, 2010).

TPS has limited use in the plastic industry because its mechanical properties depends on the humidity condition, (Bertuzzi, Castro Vidaurre, Armada, & Gottifredi, 2007; Han, 2014, chap. 9). An alternative to reduce water absorption of TPS is the chemical modification of starch before or during melt blending. When the modification is made during the extrusion, the process is known as reactive extrusion. Poly(carboxylic acid)s such as citric, tartaric and malic acids have been used as cross-linking agents and co-plasticizers to elaborate TPS. Poly(carboxylic acid)s delay water uptake, retrogradation and improve mechanical properties of TPS

* Corresponding author. Tel.: +56 41 2661216; fax: +56 41 2751233.
** Corresponding author. Tel.: +56 41 2207170; fax: +56 41 2203391.
E-mail addresses: s.rodriguez@cipachile.cl (S. Rodríguez-Llamazares), ccarrascoc@udec.cl (C. Carrasco).

[1] Bioplastic facts and figures. European Bioplastic 2013 (http://en.european-bioplastics.org/multimedia/).

http://dx.doi.org/10.1016/j.carbpol.2014.06.046
0144-8617/

(Shi et al., 2007) and are also non-toxic and of low-cost. Zuraida, Yusliza, Anuar, and Mohd Khairul Muhaimin (2012) reported the preparation of TPS from Malaysian sago and different ratios of citric acid and glycerol. TPS prepared with glycerol:citric acid ratio of 1:1 showed higher tensile strength than those prepared only with glycerol. Jiugao, Ning, and Xiaofei (2005) showed by FTIR spectroscopy and X-ray diffractometry that citric acid reduced hydrogen bonding between starch and glycerol during storage, inhibiting the formation of amylose–glycerol inclusion complexes and therefore the formation of V-type structures associated with re-crystallized starch (i.e. retrogradation). Citric, malic and tartaric acids were also used as a cross-linking agent of starch/poly(butyene adipate co-terephthalate) blends to improve the compatibility of the polymeric phase. However, these organic acids promote the hydrolysis of starch, degrading them to dextrin and fragments of low molecular weight (Olivato, Grossmann, Yamashita, Eiras, & Pessan, 2012). It would be interesting to explore the effect of malic acid on TPS plasticized by glycerol, because of its lower tendency to promote chemical modification of starch (Olivato, Grossmann, Bilck, & Yamashita, 2012; Olivato et al., 2012b; Ruxanda & Teacâ, 2012).

An attractive source of non-edible starch is the seed of horse chestnut (*Aesculus hippocastanum* L.), which a starch content over 35 wt.% (Čukanović et al., 2011). The horse chestnut was introduced in Chile around XVIII century with arrival of European immigrants, and due to its exceptional adaptability has spread throughout the whole country. It is often found as ornamental trees in urban communities and in grassland of Chilean fields. Currently, seeds of *A. hippocastanum* are used for ornamental purposes, but most of them end up in landfills. Most reports related to seeds of *A. hippocastanum* are focused on their biochemical composition and morphoanatomical character; however, we have not found detailed studies about the chemical and physical characteristics of *A. hippocastanum* starch.

In this work, *A. hippocastanum* starch was characterized and used to prepare TPS by the melt blending method. We studied the rheological, mechanical and thermal properties of this TPS and the effect of incorporating malic acid as co-plasticizer. In addition, we compared the morphological and mechanical properties of TPS from *A. hippocastanum* starch with TPS from starch of *Araucaria araucana* seeds, an edible source with C-type semi-crystalline structure and excellent precursor for starch-based materials with adequate performance (Castaño, Bouza, Rodríguez-Llamazares, Carrasco, & Vinicius, 2012).

2. Experimental

2.1. Materials

Starch of ripe *A. hippocastanum* seeds, collected at the campus of the University of Concepción, Chile, was isolated by the wet milling method. The plasticizers used were glycerol (99.5% purity) and DL-malic acid (99% purity) supplied by Oceanquímica S.A. (Valparaíso, Chile) and Sigma Aldrich (Santiago, Chile), respectively.

2.2. Characterization of A. hippocastanum starch

Physical–chemical and morphological features of *A. hippocastanum* starch granules are summarized in Table 1. Ash and moisture content were determined gravimetrically in triplicate according to ASTM D1102-56 and Chilean Standard 176/1 of 84, respectively. Nitrogen content was assessed by using Kjendhal technique (AOAC, 1990). Swelling power (g/g of starch on dry weight) and solubility (g/g of starch on dry weight) were determined in triplicate using the method reported by Singh, McCarthy, Singh, Moughan, and Kaur (2007). In short, a suspension of *A. hippocastanum* starch was heated at 60 °C for 30 min followed by centrifugation at 4000 rpm for 30 min. The supernatant was decanted and dried over night at 70 °C (soluble solid). The solid residue of centrifugation was weighed for swelling power measurement.

Table 1
Physico-chemical and morphological features of *A. hippocastanum* starch.

% Small granule size (0.5–10 μm)[a]	30.7
% Medium granule size (11–30 μm)[a]	67.6
% Large granule size (>31 μm)[a]	1.7
Moisture content[b]	7.1 ± 0.1
Ash content	0.20
Apparent amylose content (%)	33
Nitrogen content	0.5 ± 0.1
Phosphorus content (%)	0.0118
Calcium content (%)	0.0179
Sulfur content (%)	0.0033
Potassium content (%)	0.0465
Swelling power (g/g of starch on dry weight)	6.5 ± 0.2
Solubility (g/g of starch on dry weight)	3.1 ± 0.1
Color	White

[a] Determined by laser diffraction particle size analyzer.
[b] Determinated by thermogravimetric analyzer.

The apparent amylose content was assessed by using a colorimetric method according to EN ISO 6647 parts I and II, which is based on amylose–iodine complex formation. The absorbance was measured at 620 nm by using an UV spectrophotometer (UV mini – 1240 Shimadzu, Japan). The particle size distribution was determined with a laser diffraction particle size analyzer (Beckman Coulter LS™ 200, Brea CA, USA). At least three measurements were done to obtain the average particle size distribution curves. The phosphorus, sulfur, calcium and potassium content were quantified by X-ray fluorescence spectrometry (S4 Pioneer, Bruker-AXS, Germany). 5 g of powdered starch were mounted on prolene films, and analyzed under helium atmosphere. The results were evaluated by SpectraPlus v.1.6 spectrometer software (Socabim). Thermal stability of *A. hippocastanum* starch was evaluated by thermogravimetric analyses (TGA). Morphological of starch granules was examined with scanning electron microscopy. X-ray diffraction (XRD) was used to analyze crystalline structure of starch granules.

A. hippocastanum starch was debranched using isoamylase 3U (Megazyme International, Ireland) enzyme according to Wong and Jane (1995). The branch chain length distribution of amylopectin was analyzed according to Moraes, Alves, and Franco (2013) using high-performance anion-exchange chromatography with pulsed amperometric detector (HPAEC-PAD) system (ICS 3000, Dionex Corporation, Sunnyvale, USA) equipped with an AS40 automatic sampler. Samples were filtered (0.22 μm membrane) and injected into the HPAEC-PAD system (20 μL sample loop). The flow rate was 0.8 mL/min at 40 °C. The standard quadruple potential (E) waveform was employed with the following periods and pulse potentials: $E1 = 0.10$ V ($t_1 = 0.40$ s); $E2 = -2.00$ V ($t_2 = 0.02$ s); $E3 = 0.60$ V ($t_3 = 0.01$ s); $E4 = -0.10$ V ($t_4 = 0.06$ s). All eluents were prepared with ultrapure water (18 mΩ cm) with N_2 sparging. Eluent A was 150 mM NaOH and eluent B was 500 mM sodium acetate and 150 mM NaOH. The branched chains of amylopectin were separated using a Dionex CarboPacTM PA-100 guard column (4 × 50 mm) and a Dionex CarboPacTM PA-100 column (4 × 250 mm). The gradient of eluent B was 28% at 0 min, 40% at 15 min, and 72% at 105 min. The data were analyzed using the Chromeleon software, version 6.8 (Dionex Corporation, USA). The analyses were performed in duplicate.

2.3. Preparation of thermoplastic starch

Before melt-blending, *A. hippocastanum* starch and plasticizers were premixed by hand at room temperature. A Brabender internal mixer (Plastograph® EC plus, Mixer 50EHT32, Germany) was used

Table 2
Composition, rheological and tensile properties of TPS.

Sample code	*A. hippocastanum* starch (wt.%)	*A. araucana* starch (wt.%)	Malic acid (wt.%)	Glycerol (wt.%)	Torque maximum (N m)	Plasticization energy (N m/min)	Steady state (N m)	Tensile modulus (MPa)	Tensile strength (MPa)	Elongation at break (%)
CG-30	70	–	–	30	30.5	9.0	15.1	3.0 ± 0.3[a] 1.5 ± 0.2[b] 0.3 ± 0.2[c]	1.5 ± 0.1	1.02 ± 0.04
CG-MA-30	70	–	15	15	38.5	14.6	6.8			
PG-30	–	70	–	30	22.8	8.8	17.4	4.0 ± 0.5[a] 2.0 ± 0.3[b] 0.8 ± 0.2[c]	2.4 ± 0.2	1.14 ± 0.07
PG-MA-30	–	70	15	15	31.5	10.9	4.4			

[a] 10%.
[b] 30%.
[c] 90% at unitary deformation of strain.

to prepare TPS. The samples were blended at 120 °C and 60 rpm for 15 min and torque variation as a function of time was recorded. The torque values of maximum peak and steady state, and the plasticization energy were determined from the torque rheometer data (see Table 2). The integral of the torque curve, from time zero (when all the components were in the mixing chamber) to the time where the maximum torque is reached, was reported as the plasticization energy (Castaño, Rodríguez-Llamazares, Carrasco, & Bouza, 2012).

Samples were labeled specifying the type of starch and the type and wt.% of the plasticizer agent. For example, in the label CG-MA-30 C corresponded to *A. hippocastanum* starch, G to glycerol, MA to malic acid and 30 to the wt.% of plasticizers used to prepare TPS, i.e. in this case 15 wt.% of glycerol and 15 wt.% of malic acid. Table 2 summarizes composition of thermoplastic starch.

CG-30 and PG-30 samples for tension tests were injection-molded by using a Minijet II (Haake Thermo Scientific, Waltham, USA), under the following conditions: 130 °C of cylinder temperature, 55 °C of mold temperature, and 300 bar of injection pressure. To compare mechanical and morphological properties of TPS from *A. hippocastanum* and from *A. araucana*, the latter was prepared using the same condition as described above.

2.4. Characterization of thermoplastic starch

2.4.1. Scanning electron microscopy (SEM)

Morphology of *A. hippocastanum* starch granules and of cryogenically fractured surface of the mechanical test specimens of TPS obtained by injection molding (sputtered with a gold coating of ca. 50 nm) were observed at 200×, 600× and 1000× magnifications with a field emission scanning electron microscope (JEOL JSM 6380 LV, Tokyo, Japan) operated at 15 kV.

2.4.2. Thermogravimetric analysis (TGA)

Thermal stability of *A. hippocastanum* starch and TPS was evaluated using a thermogravimetric analyzer NETZSCH 209 F3 TGA (Tarsus, Selb, Germany). TGA tests were carried out at 10 °C/min under nitrogen atmosphere (20 mL/min), from 30 to 900 °C for *A. hippocastanum* starch and from 30 to 600 °C for TPS.

2.4.3. X-ray diffraction (XRD)

X-ray diffraction analysis of *A. hippocastanum* starch and TPS was performed using a Bruker Endeavour diffractometer (model D4/max-B, Germany) with Cu Kα radiation (40 kV and 20 mA). The spectra were recorded over a 2θ range of 4–35° at steps of 0.02° and time per step of 0.02°/s. Peak fitting analysis was done using a Gaussian distribution function. Degree of crystallinity was calculated using the method reported by Frost, Kaminski, Kirwan, Lascaris, and Shanks (2009).

2.4.4. Fourier transform infrared spectroscopy (FTIR)

The FTIR spectra of *A. hippocastanum* starch and TPS were recorded in triplicate at room temperature with a Jasco FTIR 4100 spectrophotometer (USA) in the range of 4000–600 cm^{-1} at 2 cm^{-1} resolution. The background and sample spectra were scanned 64 times in transmittance mode. About 5 mg of finely ground solid sample was ground with 90 mg of dry potassium bromide and a 7 mm pellet was formed under high pressure. Data was analyzed with spectral manager Version 2. The data preprocessing consisted of smoothing and manual baseline correction. For comparison, the spectra were normalized by using the band at 1459 cm^{-1}, related to the symmetric deformation of CH_2 of starch (Cael, Koenig, & Blackwell, 1975), which does not change with treatment (Morán, Vázquez, & Cyras, 2013).

2.4.5. Tensile properties

Tensile tests were performed according to ASTM D638 standard on a Karg Industrietechnik universal testing machine (Krailling, Germany) using a type V dumbbell specimen. The crosshead speed was set at 5 mm/min. Tensile strength, percent of elongation at break and Young's modulus at 10%, 30% and 90% of strain were calculated from the stress–strain curves. At least 7 individual measurements were carried out for each formulation.

3. Results and discussion

3.1. Characterization of A. hippocastanum starch

Starch granules of *A. hippocastanum* seed accumulate fundamentally in parenchyma cells of cotyledons. The size of oval parenchyma cells found was around 86 μm, considering only the large part of the cells (see complementary information, Fig. A1). This value is similar to the value reported by Musatenko, Generalova, Martyn, Vedenicheva, and Vasyuk (2003) for parenchyma cells of mature *A. hippocastanum* seeds collected in Kiev, Ukraine. Inside cells, a fiber network associated to cytoskeletal elements was also observed.

Fig. 1 shows a SEM image and the size distribution of starch granules isolated from *A. hippocastanum*. Starch granules in parenchyma cells are of diverse shape and size. The size of granules is linked to their shape, thus, small granules (0.7–9.5 μm) are spherical, the medium (10–17 μm) are oval and the larger size (18–35 μm) are irregular (for 620 granules counted). The granule surface is smooth without pores and erosion. A typical bimodal size distribution of *A. hippocastanum* starch granules is shown in Fig. 1B. Around 10% of granules have sizes between 0.4 and 3.5 μm (first interval) and the remainder granules ranged from 3.6 to 37 μm (second interval). Only 5% of granules are over 30 μm in size.

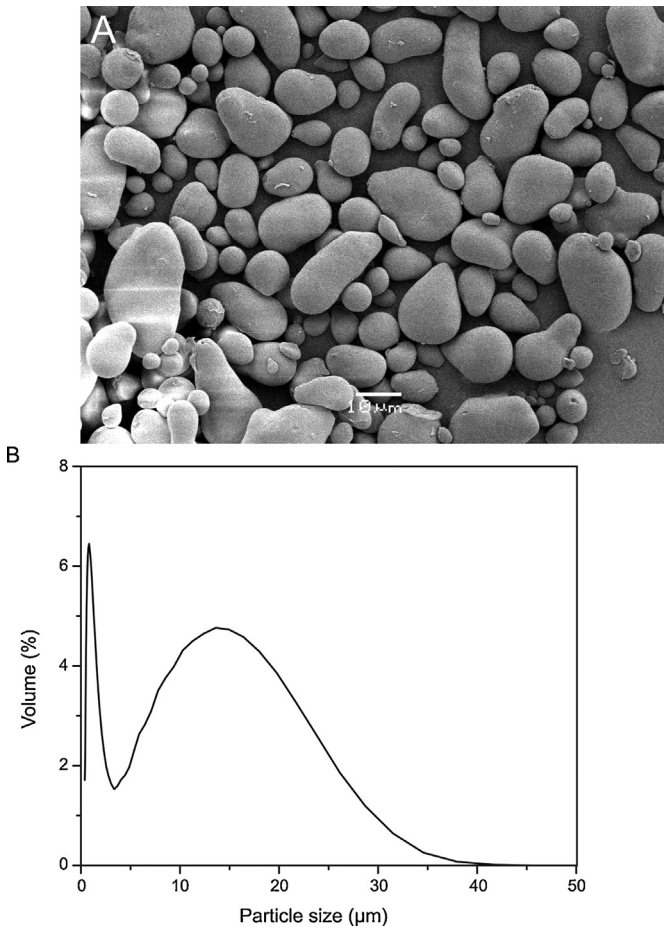

Fig. 1. (A) SEM micrograph and (B) particle-size distribution of *A. hippocastanum* starch.

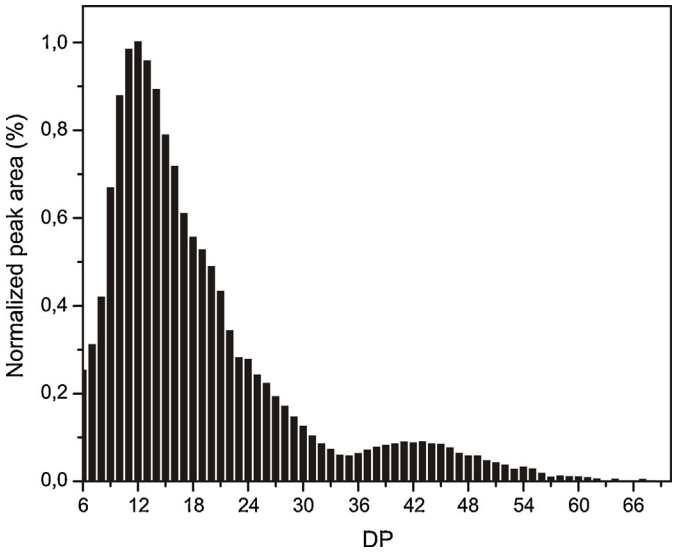

Fig. 2. Profile of amylopectin branch chain length distribution of *A. hippocastanum* starch analyzed by HPAEC-PAD.

The apparent amylose content of isolated *A. hippocastanum* starch was (33.1 ± 0.1%), considerably higher than the 14.2% and 13.8% of coarse granules and fine granules, respectively, of *A. hippocastanum* starches from Bratislava, Slovak reported by Hricovíniová and Babor (1992). The differences in amylose content can be attributed to their different source and cultivar zone, the starch isolation procedure, and the analytical methods used. They used dimethyl sulfoxide in the isolation procedure and the amylose content was determined biamperometrically by sorption of iodine.

In Fig. 2 a normalized HPAEC-PAD chromatogram shows the branch chain length distribution of amylopectin from *A. hippocastanum* starch. There are two peaks, the first one at DP = 12 (the most abundant branch unit chain) and the second one at DP 41–43. A shoulder at DP 18–22 is also observed. Average DP of branch chains of amylopectin was 18.89 ± 0.05. The proportion of amylopectin unit chains of DP 6–12, 13–24, 25–36 and ≥37 were 31.51%, 48.08%, 10.85% and 9.56%, respectively. Previous work showed correlations among chain length distribution of amylopectin and crystalline structure of starch, granule size, swelling power or gelatinization temperature. Singh et al. (2012) found that low size granules of 10–30 μm from different rice bean lines contained higher amount of DP 11–20 branch unit chains of amylopectin than large size granules of 30–105 μm. Around 53% of branch unit chains of *A. hippocastanum* starch showed a DP of 11–20, characteristic of small size granules.

The type of semi-crystalline structure of starch granules depends on the DP of external branch chains of amylopectin (Jane, 2009, chap. 6). A-type starches have a larger proportion of short B1- and A-chains, which are located, with their ends free and unrestricted, in one cluster. B-type starches have longer B-chains (B2-, B3- and B4-chains) that may extend through multiple clusters and are restricted in their movements. Jane et al. (1999) analyzed branch chain-length of amylopectin of starch isolated from different botanical sources and found some trends of branch chain-length distribution for starches with the same crystalline type. A-type starches had 15.6–27.4% of short chains (DP 6–12) and 6.6–26.7% of long chains (DP > 37), in contrast to B-type starches that had 8.5–12.3% and 26.1–29.5% of short and long chains, respectively. Similar results were reported by Srichuwong, Sunarti, Mishima, Isono, and Hisamatsu (2005a), but with 26.4–36.3% (narrower range) of branch chains with DP 9–12 for A-type starches. *A. hippocastanum* starch displayed substantial amounts of short chains of DP 6–12 (31.5%) and very few long chains (9.6%), showing a diffraction pattern characteristic of semi-crystalline structure of type C, as will be discussed later. Each starch displays its own chain-length distribution profile of amylopectin, and therefore it is not surprising that *A. hippocastanum* starch is not following the trend found by Jane et al. (1999). The proportion of each branch chain and average chain length of *A. hippocastanum* starch was within the range reported for other C-type starches (Chung & Liu, 2012).

The values of swelling power and solubility of *A. hippocastanum* starch are shown in Table 1. The ability of starch to swell in excess water, as well as its solubility, is mainly related to variations in chain branch length distribution of amylopectin and phosphorus content. Srichuwong, Sunarti, Mishima, Isono, and Hisamatsu (2005b) proposed that swelling power is associated with the unit-chain ratio (APC) of amylopectin, i.e. the ratio of relative molar distribution of amylopectin unit-chains with DP 6–12 to that of DP 6–24. A larger proportion of short chains increased the swelling power of starch granules, due to short chains forming short and weak double helices, decreasing the stability of crystalline packaging. The APC ratio of *A. hippocastanum* starch was 0.396, similar to starch granules of lesser yam, which had C-type structure and its swelling power at 70 °C was around 8 g/g.

The difference in swelling properties among starches is also attributed to phosphorus compounds, such as phospholipids and phosphate monoesters. Phospholipids form water insoluble complexes with amylose during heating, retarding starch granule swelling, while phosphate monoesters on long-branch chains of amylopectin decrease the interaction between double helices, facilitating water penetration and therefore granular swelling. The

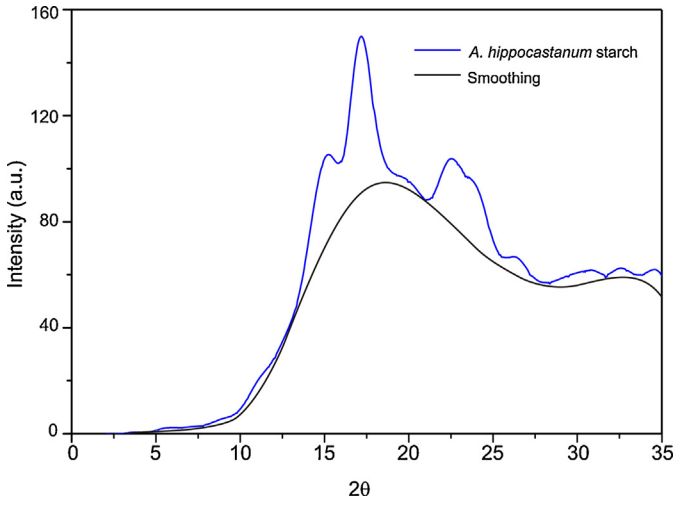

Fig. 3. X-ray diffraction pattern of *A. hippocastanum* starch.

average total phosphorus content of starch from *A. hippocastanum* was 0.0118%. This value was higher than that reported for starch from *Aesculus assamica* (0.0016%) cultivated in India (Soni, Sharma, & Bisen, 1989), both belonging to the same genus. It is interesting to observe that the swelling power of *A. hippocastanum* starch is twice of that of *A. assamica* starch, which tentatively can be attributed to the lower P content of the latter. Unfortunately, we found no reports about branch chain length distribution of amylopectin isolated from *A. assamica.*

The X-ray diffraction pattern of *A. hippocastanum* starch is shown in Fig. 2. *A. hippocastanum* starch displays a characteristic C-type pattern with diffraction peaks at $2\theta = 5.7^\circ$, 15.4°, 17.2°, 22.0° and 22.7°. The C-type pattern is not characteristic of all starches from the seed of genus *Aesculus*. For example, starch from *Aesculus indica* shows an A-type pattern (Wani et al., 2014). The degree of crystallinity of *A. hippocastanum* starch was calculated using a simple, quick and objective method (Frost et al., 2009). Amorphous background scattering was estimated using an iterative smoothing algorithm. The value of degree of crystallinity found was 10.7%, which is lower than that of starch from *A. Araucana* (15.1%) (Castañoet al., 2012a). Both starches have a C-type structure and the degree of crystallinity was calculated using the same values of polynomial order, number of iteration and point of window.

Thermal stability of native *A. hippocastanum* starch was analyzed by TGA. Fig. 3 shows the TGA and derivative of the TG curves (DTG) of starch in the temperature range of 20–900 °C. The TGA/DTG curves revealed three-steps of decomposition. The small weight loss (around 7%) between 30 and 140 °C was attributed to the evaporation of water from starch granules. The percentage of weight loss in this step was similar to the moisture content of *A. hippocastanum* starch determined gravimetrically. After 240 °C the weight loss rate quickly increased and two degradation steps were distinguished at 249 and 317 °C with a weight loss of 5.5% and 38.4%, respectively. The third degradation step between 289 and 400 °C was attributed to intermolecular dehydration to levoglucosan and some volatile products, such as carbon dioxide, lower aldehydes, methylfuranes, and ketones. The residue at 900 °C of around 10%, probably belongs to char of oxidized organic matter and inorganic substances, such as calcium, sulfur and potassium, detected by X-ray fluorescence spectrometry.

FTIR spectrum of *A. hippocastanum* starch in the 2000–800 cm^{-1} region is shown in Fig. 5. Starches from different botanical sources have similar FTIR spectra and the absorption bands have been assigned in many previous reports (Cael et al., 1975; Santha, Sudha, Vijayakumari, Nayar, & Moorthy, 1990). The broad band at 3416 cm^{-1} was assigned to O–H stretching vibration and the sharp band at 2930 cm^{-1} to C–H bond stretching of methine group of glucose rings. The band at 1646 cm^{-1} was attributed to δ(O–H) bending vibration of water. The bands at 1459 and 1419 cm^{-1} were assigned to the bending vibrations of methylene group and the band at 1369 cm^{-1} was ascribed to C–H symmetric bending vibration of methyl group. The stretching vibration bands of C–C and C–O appears in the region at 1300–800 cm^{-1}. Their intensity has been related to amorphous and crystalline phases of starch. In particular, the intensity of band at 1019 cm^{-1} decreases with increasing of amorphous state (van Soest, Tournois, de Wit, & Vliegenthart, 1995).

3.2. Characterization of TPS from A. hippocastanum starch

3.2.1. Evaluation of processability by torque rheometry

The torque-rheometer plots as a function of time showed three steps for TPS: an increasing torque from the beginning until a maximum value is reached, attributed to a plasticization process, followed by a stage of continuously decreasing values, and finally the steady state. The torque values of maximum peak and steady state, and the plasticization energy are summarized in Table 2.

TPS prepared from *A. hippocastanum* starch had higher plasticification energies and maximum torques than those from *A. araucana* starch. The type of plasticizer employed in the preparation of TPS also affected the values of plasticization energy and torque in steady state; plasticization energy was higher for glycerol:malic acid plasticized TPS than for glycerol plasticized. TPS with malic acid presented the higher viscosity (first and second step) due to the reduction of mobility of the polymeric chains as a result of chemical modification of starch by malic acid. Olivato et al. (2012a) reported that multifunctional organic acids, such as malic acid, were able to interact with the hydroxyl groups of starch; carboxyl and ester groups were formed during reactive extrusion, promoting esterification and trans-esterification reactions of starch.

Once starch granules were destructurized, the torque decreased until reaching a steady state. CG-MA-30 and PG-MA-30 samples showed the lowest torques in steady state (see Table 2), because multifunctional organic acids also promote the acid hydrolysis of the glycosidic linkages of starch, decreasing the molecular weight of amylose and amylopectin, as well as the degree of polymerization of the amylopectin molecules (Da Róz, Zambon, Curvelo, & Carvalho, 2011). Similar behavior of rheological properties was reported by Jiugao et al. (2005) for glycerol plasticized starch modified with citric acid.

On the other hand, the time required to reach steady state depended on the type of plasticizer and type of starch (see Fig. A2). The time was around 4 min for samples without malic acid, 8 min, for the CG-MA-30 sample, and 11 min for the PG-MA-30 sample. Glycerol:malic acid plasticized TPS showed a slight downward trend with time in steady state, indicating a continuous but small change in viscosity of these samples. The reduction of viscosity of TPS with malic acid is attributed not only to the decrease of molecular weight of starch, but also to less branch chains of amylopectin participating in the formation of entanglements structures with the outer chains of other amylopectin, or with amylose (van Soest et al., 1996).

3.2.2. Scanning electron microscopy

SEM images of the fractured surfaces (Fig. 6) displayed continuous phases. However, some broken starch granules were detected in the rough fractured surface of the CG-30 sample (Fig. 6A). The broken granules were completely embedded in the TPS matrix. No signs of granule pullout and pits on the surface, and no obvious

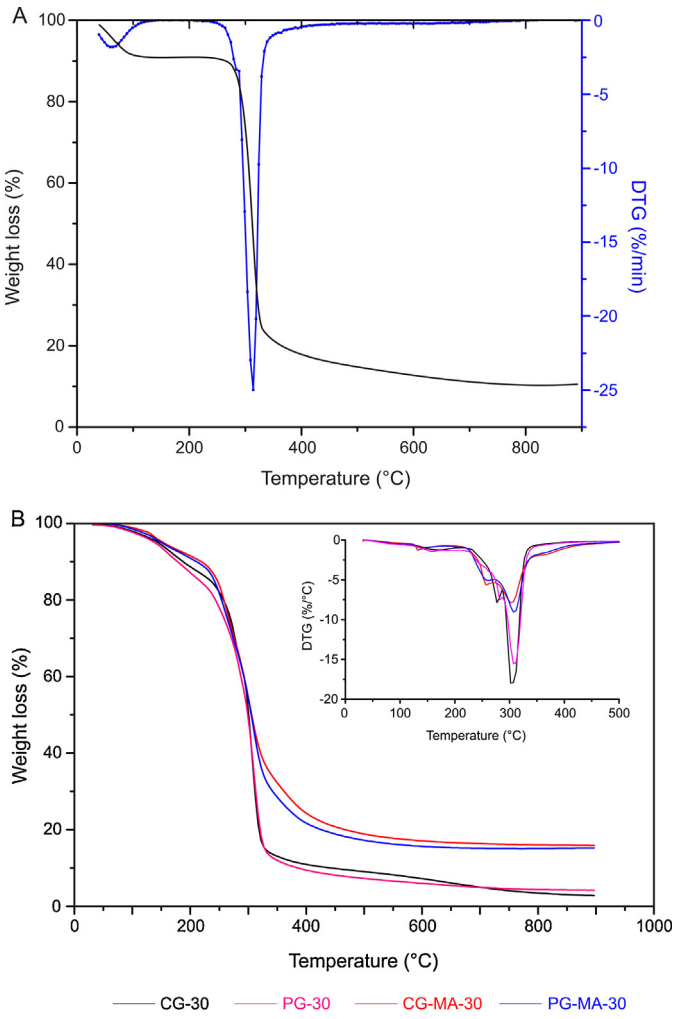

Fig. 4. TGA and DTG curves of (A) *A. hippocastanum* starch and (B) TPS.

gaps at the irregular interfaces between the broken granule and the matrix were observed. Thus, the addition of 30 wt.% of glycerol in the CG-30 sample was not enough for achieving complete plasticization of TPS under used processing conditions. Similar results were reported by Qiao, Tang, and Sun (2011) and Mao, Imam, Gordon, Cinelli, and Chiellini (2000). As reported previously the PG-30 sample exhibited a rough and homogenous surface without granules (Castaño et al., 2012b).

CG-MA-30 and PG-MA-30 samples presented smooth and homogenous fractured surfaces with some randomly distributed holes. Ma, Chang, Yu, and Stumborg (2009) reported that pits found in fractured surface of glycerol:citric acid plasticized TPS were due to exfoliation of non-destructured starch granules. However, fragments or entire granules were not observed at the surface of these samples, as expected for concentrations of organic acids higher than 1 wt.%, which promote the disruption and dissolution of starch granules (Jiugao et al., 2005).

3.2.3. Thermal stability

TGA curves of TPS exhibited similar behavior with three steps of decomposition (Fig. 4B). Loss weight varied slowly from room temperature up to 100 °C, with a weight loss of about 2%. The maximum decomposition temperature (T_{max}) and associated weight loss at each decomposition step depended on starch source and plasticizer used. Glycerol:malic acid plasticized TPS exhibited lower thermal stability than TPS prepared with glycerol alone, due to a reduction of molecular weight of starch chains by acid hydrolysis (Jiugao et al., 2005).

Thermal degradation at the first step of decomposition was associated to loss of low molecular weight substances such as water and glycerol. T_{max} of first step of CG-30 sample (176.9 °C) was higher than that of PG-30 (156.9 °C) due to the lower water content of *A. hippocastanum* (7.0 wt.%) compared to *A. araucana* (8.1 wt.%). With decreasing water content of TPS the boiling point of glycerol–water mixture increases. This behavior is more pronounced at weight fraction of water lower than 10 wt.% in water/glycerol mixtures (Chen & Thompson, 1970). The second decomposition peak appeared in the range of 277–282 °C for TPS prepared with glycerol and in the range of 257–262 °C for glycerol:malic acid plasticized TPS, and was mainly associated to evaporation of glycerol. Note that weight loss at T_{max} of second peak was one-third less in glycerol:malic acid plasticized TPS. After 300 °C the weight loss corresponds to dehydration and decomposition of starch (Liu, Xie, Yu, Chen, & Li, 2009). As expected, the values of T_{max} of the third step only depended on starch source, being 301.9 and 306.9 °C for TPS prepared with *A. hippocastanum* starch and with *A. araucana* starch, respectively.

The residual weight percentage of TPS prepared with glycerol:malic acid was higher than those prepared with glycerol. Similar results were reported by Shi et al. (2007). They attributed the increasing of residual weight to the tendency of char formation of esterified starch.

3.2.4. FTIR analysis

The changes in FTIR spectra between 2000 and 800 cm^{-1} of *A. hippocastanum* starch plasticized with glycerol alone and with glycerol:malic acid by melt blending are shown in Fig. 4. The intensity of bands between 1200 and 950 cm^{-1} decreased in TPS, due to the destructuration and decreasing crystallinity of starch (van Soest et al., 1995). In particular, the band at 1019 cm^{-1}, associated to C–O bond of C–O–C in starch (Jiugao et al., 2005), was not observed in CG-30 and CG-MA-30 spectra. However, the band at 1052 cm^{-1} (shoulder in FTIR spectrum of *A. hippocastanum* starch) was shifted to a lower wave numbers in CG-30 (1039 cm^{-1}) and CG-MA-30 (1035 cm^{-1}) samples. The shift of band at 1052 cm^{-1} to lower wave numbers (around 13 cm^{-1}) in TPS prepared with glycerol could be due to the formation of hydrogen bonds among C–O–H and C–O–C groups of starch and OH of glycerol. In glycerol:malic acid plasticized TPS this shift was higher (around 17 cm^{-1}), probably due to hydroxyl and carboxyl groups of poly(carboxylic acid) interacting stronger with C–O–H and C–O–C groups in starch than with glycerol. A new strong band appeared at 1739 cm^{-1} on FTIR spectrum of CG-MA-30 sample, which corresponds to C=O ester carbonyl group stretching. The peak at 1739 cm^{-1} is associated to the ester bond in esterified starch (Diop, Li, Xie, & Shi, 2011; Ma et al., 2009).

3.2.5. Tensile properties

The effect of starch source (*A. hippocastanum* and *A. araucana*) on the tensile properties of glycerol plasticized TPS is shown in Table 2, where tensile modulus, tensile strength and elongation at break of TPS are summarized. Note that tensile modulus, i.e. tangent modulus, was calculated at 10%, 30% y 90% of strain, because the samples did not present Hookean behavior. PG-30 compared with CG-30 exhibited higher values of tensile properties. Tensile strength was 60% and tensile modulus at high deformation of strain was almost 200% higher; the rigidity and higher strength of PG-30 was associated to the absence of residual starch granules at fractured surfaces (Fig. 6B) and the higher apparent amylose content of *A. araucana* starch. Chaudhary, Torley, Halley, McCaffery, and Chaudhary (2009) studied the effect of amylose content on tensile properties of TPS from maize obtained by melt blending, and concluded that high amylose TPS tend to be tougher due to the higher

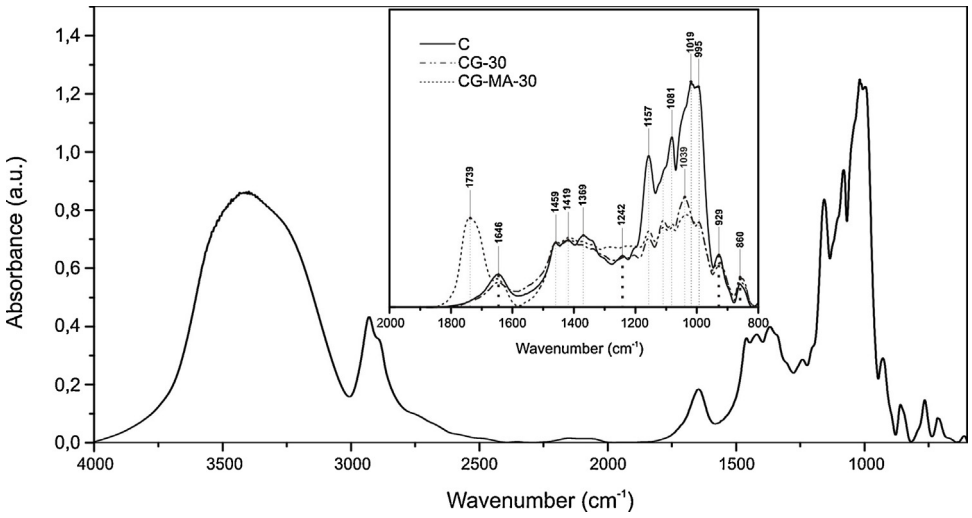

Fig. 5. FTIR spectrum of *A. hippocastanum* starch and TPS.

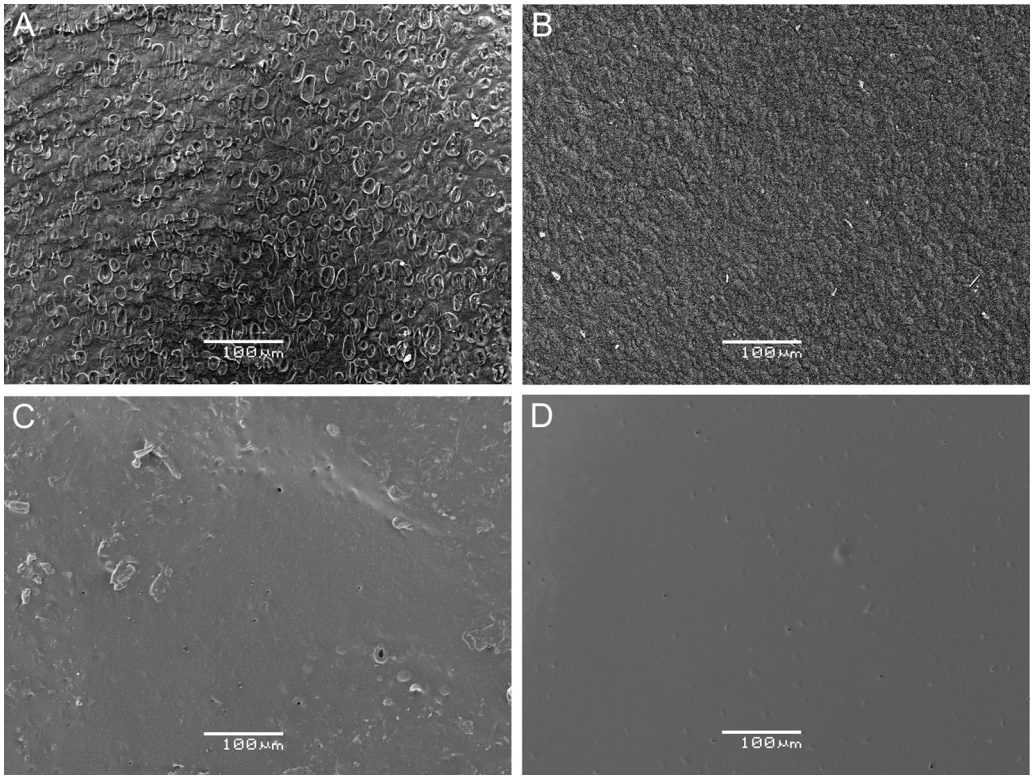

Fig. 6. SEM micrographs of fracture surfaces of molded TPS specimens: (A) CG-30; (B) PG-30; (C) CG-MA-30 and (D) PG-MA-30.

degree of interactions among the double helix structure of amylose and the outer chains of amylopectin. The entanglement between amylose and amylopectin gave a TPS material with a denser polymer network.

Glycerol:malic acid plasticized TPS prepared exhibited a sticky behavior, making it impossible to remove the specimens from the mold without plastic deformation. The sticky behavior was attributed to the fact that malic acid (15 wt.%) promoted acid hydrolysis of the glycosidic linkages in starch. Da Róz et al. (2011) correlated the reduction of viscosity and the stickiness of TPS prepared with glycerol:water:poly(carboxylic acid) with the decrease of molecular weight in starch.

4. Conclusion

A. hippocastanum L. seed is an attractive source of non-edible starch for the production of starch-based materials. This seed is easily collected and presently ends up in landfills. Starch isolated from *A. hippocastanum* seed shows a bimodal size distribution with characteristic shapes for each mode. *A. hippocastanum* starch displayed a typical C-type diffraction pattern. The high swelling power of this starch is due to the proportion of short branch chains of amylopectin (APC ratio = 0.396) and phosphorous content (0.012%).

Glycerol plasticized TPS from *A. hippocastanum* and from *A. auracana* starch showed similar rheological and thermal properties.

Tensile strength and young modulus were lower for TPS from *A. hippocastanum*. The fractured surface of glycerol plasticized TPS from *A. hippocastanum* starch displayed residual starch granules.

The use of malic acid at 15 wt.% as co-plasticizer adversely affected thermal and mechanical properties of TPS plasticized by glycerol. Glycerol:malic acid plasticized TPS exhibited pasty and sticky behavior, which can be attributed to increasing depolymerization of starch molecules by acid hydrolysis promoted by malic acid.

Acknowledgments

This work has been financed by CONICYT-REGIONAL R08C1002 and Programa de Financiamiento Basal para Centros Científicos y Tecnológicos de Excelencia PFB-27, Projects InnovaChile 13IDL2-23120 and Fondef D09I1195.

Appendix A.

See Figs. A1 and A2.

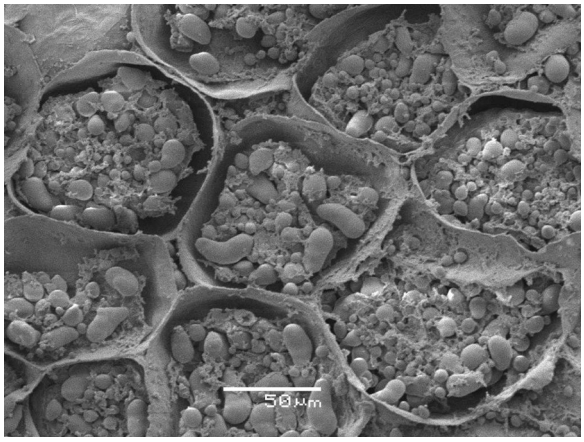

Fig. A1. Storage parenchyma cells from cotyledon of mature *A. hippocastanum* seed.

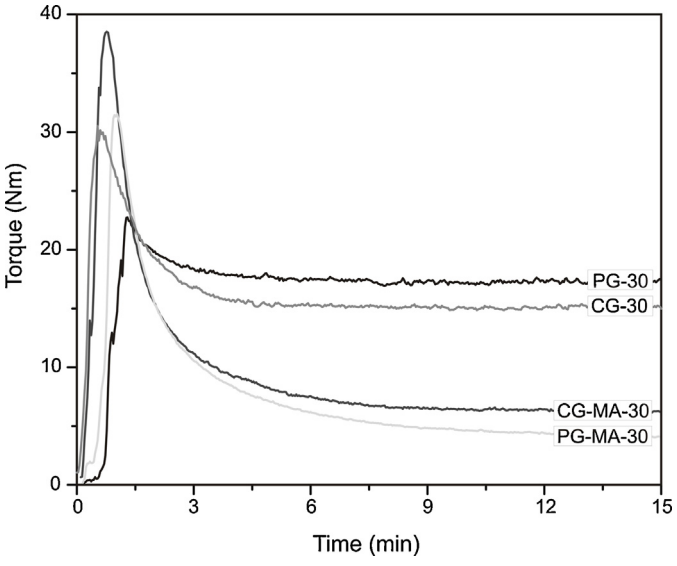

Fig. A2. Torque variation as a function of time for TPS.

References

Bertuzzi, M. A., Castro Vidaurre, E. F., Armada, M., & Gottifredi, J. C. (2007). Water vapor permeability of edible starch based films. *Journal of Food Engineering*, *80*(3), 972–978.

Bharadwaj, D. N. (2010). Use and environment impact of biodegradable plastics a review. *Current Advances in Agricultural Sciences*, *2*(2), 65–69.

Cael, J. J., Koenig, J. L., & Blackwell, J. (1975). Infrared and Raman spectroscopy of carbohydrates. Part VI: Normal coordinate analysis of V-amylose. *Biopolymers*, *14*(9), 1885–1903.

Castaño, J., Bouza, R., Rodríguez-Llamazares, S., Carrasco, C., & Vinicius, R. V. B. (2012). Processing and characterization of starch-based materials from pehuen seeds (*Araucaria araucana* (Mol) K. Koch). *Carbohydrate Polymers*, *88*(1), 299–307.

Castaño, J., Rodríguez-Llamazares, S., Carrasco, C., & Bouza, R. (2012). Physical, chemical and mechanical properties of pehuen cellulosic husk and its pehuen-starch based composites. *Carbohydrate Polymers*, *90*, 1550–1556.

Čukanović, J., Ninić-Todorović, J., Ognjanov, V., Mladenović, E., Ljubojević, M., & Kurjakov, A. (2011). Biochemical composition of the horse chestnut seed (*Aesculus hippocastanum* L.). *Archives of Biological Sciences Belgrade*, *63*(2), 345–351.

Chaudhary, A. L., Torley, P. J., Halley, P. J., McCaffery, N., & Chaudhary, D. S. (2009). Amylose content and chemical modification effects on thermoplastic starch from maize – Processing and characterisation using conventional polymer equipment. *Carbohydrate Polymers*, *78*(4), 917–925.

Chen, D. H. T., & Thompson, A. R. (1970). Isobaric vapor–liquid equilibriums for the systems glycerol–water and glycerol–water saturated with sodium chloride. *Journal of Chemical & Engineering Data*, *15*(4), 471–474.

Chung, H.-J., & Liu, Q. (2012). Physicochemical properties and in vitro digestibility of flour and starch from pea (*Pisum sativum* L.) cultivars. *International Journal of Biological Macromolecules*, *50*(1), 131–137.

Da Róz, A. L., Zambon, M. D., Curvelo, A. A. S., & Carvalho, A. J. F. (2011). Thermoplastic starch modified during melt processing with organic acids: The effect of molar mass on thermal and mechanical properties. *Industrial Crops and Products*, *33*(1), 152–157.

Diop, C. I. K., Li, H. L., Xie, B. J., & Shi, J. (2011). Effects of acetic acid/acetic anhydride ratios on the properties of corn starch acetates. *Food Chemistry*, *126*(4), 1662–1669.

Frost, K., Kaminski, D., Kirwan, G., Lascaris, E., & Shanks, R. (2009). Crystallinity and structure of starch using wide angle X-ray scattering. *Carbohydrate Polymers*, *78*(3), 543–548.

Han, J. H. (2014). Edible films and coatings: A review. In J. H. Han (Ed.), *Innovations in food packaging* (2nd ed., pp. 213–255). San Diego: Academic Press.

Hricovíniová, Z., & Babor, K. (1992). Saccharide constituents of horse chestnut (*Aesculus hippocastanum* L.) seeds II/isolation and characterization of the starch. *Chemical Papers*, *45*(3), 196–198.

Jane, J., Chen, Y. Y., Lee, L. F., McPherson, A. E., Wong, K. S., Radosavljevic, M., et al. (1999). Effects of amylopectin branch chain length and amylose content on the gelatinization and pasting properties of starch. *Cereal Chemistry Journal*, *76*(5), 629–637.

Jane, J.-L. (2009). Chemistry and technology. In J. BeMiller, & R. Whistler (Eds.), *Structural features of starch granules II* (3rd ed., pp. 205–225).

Jiugao, Y., Ning, W., & Xiaofei, M. (2005). The effects of citric acid on the properties of thermoplastic starch plasticized by glycerol. *Starch – Stärke*, *57*(10), 494–504.

Liu, H., Xie, F., Yu, L., Chen, L., & Li, L. (2009). Thermal processing of starch-based polymers. *Progress in Polymer Science*, *34*(12), 1348–1368.

Ma, X., Chang, P. R., Yu, J., & Stumborg, M. (2009). Properties of biodegradable citric acid-modified granular starch/thermoplastic pea starch composites. *Carbohydrate Polymers*, *75*(1), 1–8.

Mao, L., Imam, S., Gordon, S., Cinelli, P., & Chiellini, E. (2000). Extruded cornstarch–glycerol–polyvinyl alcohol blends: Mechanical properties, morphology, and biodegradability. *Journal of Polymers and the Environment*, *8*(4), 205–211.

Moraes, J., Alves, F. S., & Franco, C. M. L. (2013). Effect of ball milling on structural and physicochemical characteristics of cassava and Peruvian carrot starches. *Starch – Stärke*, *65*(3–4), 200–209.

Morán, J. I., Vázquez, A., & Cyras, V. P. (2013). Bio-nanocomposites based on derivatized potato starch and cellulose, preparation and characterization. *Journal of Materials Science*, *48*(20), 7196–7203.

Musatenko, L. I., Generalova, V. N., Martyn, G. I., Vedenicheva, N. P., & Vasyuk, V. A. (2003). Hormonal complex and ultrastructure of maturing *Aesculus hippocastanum* seeds. *Russian Journal of Plant Physiology*, *50*(3), 360–364.

Olivato, J. B., Grossmann, M. V. E., Bilck, A. P., & Yamashita, F. (2012). Effect of organic acids as additives on the performance of thermoplastic starch/polyester blown films. *Carbohydrate Polymers*, *90*(1), 159–164.

Olivato, J. B., Grossmann, M. V. E., Yamashita, F., Eiras, D., & Pessan, L. A. (2012). Citric acid and maleic anhydride as compatibilizers in starch/poly(butylene adipate-co-terephthalate) blends by one-step reactive extrusion. *Carbohydrate Polymers*, *87*(4), 2614–2618.

Qiao, X., Tang, Z., & Sun, K. (2011). Plasticization of corn starch by polyol mixtures. *Carbohydrate Polymers*, *83*, 659–664.

Ruxanda, B., & Teacă, C. A. (2012). Effects of chemical modification on the structure and mechanical properties of starch-based biofilms. *Monatshefte für Chemie*, *143*, 335–343.

Santha, N., Sudha, K. G., Vijayakumari, K. P., Nayar, V. U., & Moorthy, S. N. (1990). Raman and infrared spectra of starch samples of sweet potato and cassava. *Journal of Chemical Sciences*, *102*(5), 705–712.

Shi, R., Zhang, Z., Liu, Q., Han, Y., Zhang, L., Chen, D., et al. (2007). Characterization of citric acid/glycerol co-plasticized thermoplastic starch prepared by melt blending. *Carbohydrate Polymers*, *69*(4), 748–755.

Singh, J., McCarthy, O. J., Singh, H., Moughan, P. J., & Kaur, L. (2007). Morphological, thermal and rheological characterization of starch isolated from New Zealand Kamo Kamo (*Cucurbita pepo*) fruit – A novel source. *Carbohydrate Polymers*, *67*(2), 233–244.

Singh, N., Kaur, S., Isono, N., Ichihashi, Y., Noda, T., Kaur, A., et al. (2012). Diversity in characteristics of starch amongst rice bean (*Vigna umbellate*) germplasm: Amylopectin structure, granules size distribution, thermal and rheology. *Food Research International*, *46*(1), 194–200.

Soni, P. L., Sharma, H. W., & Bisen, S. S. (1989). Physicochemical properties of *Careya arborea* and *Aesculus assamica* starches. *Starch – Stärke*, *41*(6), 208–211.

Srichuwong, S., Sunarti, T. C., Mishima, T., Isono, N., & Hisamatsu, M. (2005a). Starches from different botanical sources I: Contribution of amylopectin fine structure to thermal properties and enzyme digestibility. *Carbohydrate Polymers*, *60*(4), 529–538.

Srichuwong, S., Sunarti, T. C., Mishima, T., Isono, N., & Hisamatsu, M. (2005b). Starches from different botanical sources II: Contribution of starch structure to swelling and pasting properties. *Carbohydrate Polymers*, *62*(1), 25–34.

van Soest, J. J. G., Benes, K., de Wit, D., & Vliegenthart, J. F. G. (1996). The influence of starch molecular mass on the properties of extruded thermoplastic starch. *Polymer*, *37*(16), 3543–3552.

van Soest, J. J. G., Tournois, H., de Wit, D., & Vliegenthart, J. F. G. (1995). Short-range structure in (partially) crystalline potato starch determined with attenuated total reflectance Fourier-transform IR spectroscopy. *Carbohydrate Research*, *279*, 201–214.

Vieira, M., da Silva, M., dos Santos, L., & Beppu, M. (2011). Natural-based plasticizers and biopolymer films: A review. *European Polymer Journal*, *47*(3), 254–263.

Wani, I. A., Jabeen, M., Geelani, H., Masoodi, F. A., Saba, I., & Muzaffar, S. (2014). Effect of gamma irradiation on physicochemical properties of Indian Horse Chestnut (*Aesculus indica* Colebr.) starch. *Food Hydrocolloids*, *35*, 253–263.

Wong, K. S., & Jane, J. (1995). Effects of pushing agents on the separation and detection of debranched amylopectin by high-performance anion-exchange chromatography with pulsed amperometric detection. *Journal of Liquid Chromatography*, *18*(1), 63–80.

Zullo, R., & Iannace, S. (2009). The effects of different starch sources and plasticizers on film blowing of thermoplastic starch: Correlation among process, elongational properties and macromolecular structure. *Carbohydrate Polymers*, *77*(2), 376–383.

Zuraida, A., Yusliza, Y., Anuar, H., & Mohd Khairul Muhaimin, R. (2012). The effect of water and citric acid on sago starch bio-plastics. *International Food Research Journal*, *19*(2), 715–719.